Desalination and Water Treatment
www.deswater.com
doi: 10.5004/dwt.2020.24955

178 (2020) 123–135
February

Study on nano-chitosan grafting quaternary ammonium salt modified polyacrylamide for flocculation and sterilization

Zheng Zhong[a,b,§], Fengjiao Zhang[a,§], Wei Chen[a,b,*], Xiaguo Wei[a], Yiwen Zhang[a], Yanbo Lu[a], Hongbin Luo[a], Liangqian Fan[a]

[a]*College of Civil Engineering, Sichuan Agricultural University, Dujiangyan 611830, China, emails: chenwei0835@163.com (W. Chen), zhongzheng99@live.cn (Z. Zhong), 1215139045@qq.com (F. Zhang), 854015906@qq.com (X. Wei), 1374711069@qq.com (Y. Zhang), lew619906814@gmail.com (Y. Lu), luohongbing66@163.com (H. Luo), flqjacky@163.com (L. Fan)*
[b]*Sichuan Higher Education Engineering Research Center for Disaster Prevention and Mitigation of Village Construction, Department of Municipal Engineering, Chengdu 611830, China*

Received 21 April 2019; Accepted 21 September 2019

ABSTRACT

A dual-function chitosan-based flocculant named nano-chitosan-graft-poly(acrylamide and acryloyloxyethyltrimethyl ammonium chloride (NCS-g-P(AM-DAC)) with flocculation and sterilization properties was successfully synthesized by using nano-chitosan (NCS), acrylamide, and acryloyloxyethyltrimethyl ammonium chloride (DAC) under ultraviolet irradiation with 2,2′-Azobis(2-methylpropionamidine) dihydrochloride as the photo-initiator. NCS was obtained via ion cross-linking between chitosan and sodium tripolyphosphate. The structure and physicochemical properties of the product were characterized by various methods. The influence of different factors on the intrinsic viscosity of synthetic copolymer was investigated to optimize the synthetic condition. The flocculation performance of NCS-g-P(AM-DAC) was evaluated. Results showed that the superior flocculation efficiency was acquired under pH = 6 and flocculant dosage of 5 mg L^{-1}, in which turbidity removal efficiency was above 85%. Considering that the quaternary ammonium salt was grafted and the nanoparticle generated, NCS-g-P(AM-DAC) was also applied to flocculate *Escherichia coli (E. coli)* suspension to evaluate the sterilization performance. At suitable dosage and pH conditions, the flocculant effectively removed turbidity and bacterial cells. 3D fluorescence spectroscopy analysis of *E. coli* suspension after the flocculation was conducted to investigate the sterilization mechanism. The results showed that NCS-g-P(AM-DAC) could destroy cell membranes, indicating its bactericidal, not simply antibacterial, effect during flocculation.

Keywords: Nano-chitosan; Turbidity removal; Grafting; Dual-function; Flocculation; Sterilization

1. Introduction

Water pollution has now become a severe environmental problem worldwide, and as a consequence, water resources shortage and water contamination have become chief factors that restrict economical and societal development [1]. To solve this problem, several purification methods have been developed. Flocculation is one of the most common and important conventional water treatment technologies for the purification process because of its convenience and cost-saving performance [2]. Aggregation and settlement are the two basic processes of flocculation, in which the formed flocs can be separated from the wastewater. The flocculation process is considered to be one of the most important parts that play a decisive role in the whole water treatment. Therefore, the flocculant efficiency greatly affects the water quality, treatment cost, and the subsequent purification [3,4]. Suspended

* Corresponding author.
§ These authors contributed equally to this work and should be considered as co-first authors.

colloidal particles in wastewater deteriorate water quality and provide habitats for microorganisms, resulting in the breeding of pathogens, such as *Escherichia coli (E. coli)* that affects people's health. The suspended colloidal particles are always removed by flocculants during flocculation, and the microorganisms are eradicated by bactericides during sterilization. To control the number of microorganisms, the bactericides are always added to each unit, possibly leading to the high cost and secondary pollution by bactericide by-products that show potential health risks to the human body [5]. Considering the complexity of wastewater composition and the shortcomings of traditional water treatment, the synthesis, and employment of highly efficient, economical, multifunctional flocculants have become a hot topic in this field [6]. At present, traditional inorganic and synthetic polymers flocculants are commonly used. However, it was reported that they may be potentially harmful to health and cause secondary pollution during the treatment process [7]. It was also researched that traditional inorganic and synthetic polymer flocculants showed less activity for disinfection [8]. Thus, novel environmentally friendly materials for flocculation are undoubtedly needed. The society pays increasing attention to natural polymer flocculants due to their environmental friendliness and ample existence in nature.

Chitosan (CS), as the second most abundant natural organic resource and natural cationic adsorbent [9], can be widely found in the shells of crustaceans such as shrimp and crabs and is non-toxic, tasteless, alkali resistant, biocompatible, and biodegradable [10]. Reactive functional groups, such as amino groups and hydroxyl groups, play important roles in the molecule chain of CS and determine its remarkable property [11,12]. CS is positively charged under acidic conditions because of the large positive charge of the protonated amino group. This condition is favorable for flocculation because several of the suspension colloidal particles and microorganisms in wastewater are negatively charged [13]. Nonetheless, CS is usually only dissolved in acidic solution, indicating that its molecular weight reduces greatly under acidic conditions. Additionally, the amino groups on the molecule are not strong enough for the purification of the wastewater containing complex components. The low molecular weight, low solubility, and poor mechanical properties of CS can not meet the standard in some application fields, thus limiting its application. Chemical modifications are imperative to overcome these drawbacks. As a linear polymer and a common basis modification material, polyacrylamide (PAM) is widely used as an organic flocculant because of its long branches and high intrinsic viscosity. Acryloyloxyethyltrimethyl ammonium chloride (DAC), which is also employed as a flocculant and bactericide for water treatment, is a common quaternary ammonium salt. In previous works [14,15], PAM and cationic quaternary ammonium salt were frequently selected as raw materials to synthesize copolymer flocculants to increase molecular weight and enhance electropositivity. These synthetic products exhibit prominent performance in flocculation for negatively charged suspended colloidal particles, sludge dehydration, sterilization, and other applications. The methods of modification are principally distinguished by the way of generating free radicals, including thermal initiation [16,17], gamma-ray initiation[18,19], microwave initiation[20], and ultraviolet (UV) initiation[21–23]. By comparison, UV initiation requires reasonable conditions, such as short polymerization time, few initiators, and high reaction. Also, the operability and environmental friendliness of this method make it popular.

Nanoparticle refers to tiny material with a particle size ranging from 1 to 100 nm and shows surface and interface effects, small size effects, macroscopic quantum tunneling effects, and quantum size effects due to the special structure [24]. Recently, the application of nanomaterials has been extended to flocculation, sterilization and wastewater treatments [25–27]. In previous studies, it has been demonstrated that nano-chitosan (NCS) can be obtained by specific methods and has already been applied for protein delivery and metal ion adsorption [28–30]. However, the use of NCS as a flocculant has been rarely reported because of its low molecule weight. Fortunately, NCS prepared through PAM grafting modification can compensate for the low molecular weight of increase the intrinsic viscosity and extend the molecular chain, thereby showing potentially good performance in flocculation treatment [31]. In addition, NCS is potentially employed as a nanomaterial bactericide for biological applications. Limited reports have been found on grafting PAM and DAC onto NCS and on the synthesis of CS-based flocculants with a dual function. These processes are undoubtedly an improvement in the material's properties, spreading the area of application and enriching the functions due to its special nanostructure, high molecule weight and positive charge density [32]. Meanwhile, the quaternary ammonium salt is widely studied and applied as a bactericide for water treatment sterilization [33]. The introduction of quaternary ammonium groups with a strong hydration capacity and great resistance into CS immensely weakens its intermolecular hydrogen bonds to increase its water solubility and improves its molecular weight, positive charge and its antibacterial properties [34].

With regard to these key points, CS and sodium tripolyphosphate (TPP) were used as raw materials to prepare NCS via ion cross-linking in this study. A novel, environmentally friendly, efficient dual-function flocculant nano-chitosan-graft-poly(acrylamide and acryloyloxyethyltrimethyl ammonium chloride (NCS-g-P(AM-DAC)) was synthesized through UV initiation. Its optimal synthetic preparation conditions were explored. The physicochemical properties of the obtained product were characterized by Fourier transform infrared spectroscopy (FT-IR), scanning electron microscopy (SEM), and thermogravimetric analysis/differential scanning calorimetry (TG/DSC). The particle size of various obtained flocculants was analyzed and compared according to particle size distribution. The as-synthesized material was applied to flocculate kaolin suspension samples to evaluate flocculation performance. In addition, *E. coli* removal experiment was conducted to investigate its sterilization effect. 3D fluorescence spectroscopy (3D-EEM) was employed to further study its antibacterial mechanism during flocculation.

2. Experimental parts

2.1. Materials

CS (with of deacetylation degree of 95% and viscosity of 100–200 mPas) was purchased from Shanghai Jingchun

Biotechnology Co. Ltd., (Shanghai, China). Acrylamide (AM) (analytical grade), and DAC (industrial grade) were obtained from Chongqing Lanjie Tap Water Company (Chongqing, China). Sodium (TPP, analytical grade) and 2,2′-Azobis (2-methylpropionamidine) dihydrochloride (V_{50}, analytical grade) were sourced from Shanghai Aladdin Biochemical Science Stock Company Ltd., (Shanghai, China). Hydrochloric acid (HCl), sodium hydroxide (NaOH), sodium chloride (NaCl), glacial acetic acid (HAc), acetone and ethanol, were all purchased from Kelong Chemical Reagent Co. Ltd., (Chengdu, China). All analytical grade reagents were used without further purification. Besides, LB broth was obtained from Qingdao Hopebio-Technology Co. Ltd., (Qingdao, China). *E. coli* original strain (CMCC 44102) was provided by the Institute of Microbiology, Chinese Academy of Sciences.

2.2. Preparation of NCS

The NCS was prepared via an ion cross-linking reaction in accordance with present work [29,30,35]. CS of 0.4 g was dissolved in 30 mL of 1% (wt.) acetic acid under magnetic stirring. TPP solution (5 mg mL^{-1}) of 16 mL was slowly and dropwise added into the CS solution under appropriate magnetic stirring at room temperature. The suspension was gelated for 30 min and the solution was then ultrasonically treated for 2 min to reduce the particle size. Finally, the NCS solution was obtained for subsequent NCS-g-P(AM-DAC) copolymerization.

2.3. Preparation of NCS-g-P(AM-DAC)

Solid AM of 3.2 g and DAC of 0.5 g solution (wt.% = 80%) were added into the NCS solution. After these substances were completely dissolved, V_{50} as the initiator of 1% of monomer mass was added. Nitrogen (99.99% pure) was then injected into the solution for 15 min to remove the oxygen. Subsequently, the reactor was immediately sealed and irradiated by UV illumination for 3.5 h at room temperature. After the reaction, the polymer was precipitated in the mixed solution of acetone and ethanol at a volume ratio of 2:1. The generated homopolymer during the reaction can be eliminated after washing twice or three times. Then the extractives were dried in the oven at 80°C until a constant weight was obtained. The reaction of NCS-g-P(AM-DAC) copolymerization is shown in Fig. 1.

2.4. Charaterization

NCS-g-P(AM-DAC) and other samples were characterized via FT-IR (BRUKER Company, Switzerland. At the wavenumbers of 400–4,000 cm^{-1}), SEM (ZEISS, Germany), particle size distribution, zeta potential (Malvern, UK), and TG/DSC (Shimadzu, Japan. From room temperature to 600°C with a heating rate of 10°C min^{-1} under a nitrogen flow of 20 mL min^{-1}).

2.5. Measurement of intrinsic viscosity

The intrinsic viscosity of the copolymer solution was measured by the one-point method [36] using the Ubbelohde viscometer at 30°C ± 0.5°C after filtering by a sand core funnel. Fully dried NCS-g-P(AM-DAC) of 0.06 g was ground into a powder and dissolved in 75 mL of aqueous acetic acid solution (0.1 mol L^{-1}) and sodium chloride (0.1 mol L^{-1}) at the molar ratio of CH_3COOH and NaCl of 1:2. By counting the efflux time of the solvents, the intrinsic viscosity was calculated using a reported equation as follows.

$$\eta = \frac{\left(\frac{3}{2}\eta_{sp}^2 - 3\eta_{sp} + 3\ln\eta_r\right)^{1/3}}{c} \quad (1)$$

$$\eta_r = \frac{t}{t_0} \quad (2)$$

$$\eta_{sp} = \eta_{sp} - 1 \quad (3)$$

where η_r is the relative viscosity of samples, η_{sp} is the specific viscosity, t is the efflux time of NCS-g-P(AM-DAC) solution, t_0 is the efflux time of the mixture of NaCl and CH_3COOH solution, and c is the mass concentration of NCS-g-P (AM-DAC) solution (g L^{-1}).

2.6. Flocculation experiment

The flocculation experiments were conducted in 500 mL beakers by using a program-controlled jar test apparatus (ZR4-6, Zhongrun, China). Kaolin suspension with initial turbidity of 200 ± 5 NTU was prepared, and the initial pH was adjusted by 0.1 mol L^{-1} sodium hydroxide and 0.1 mol L^{-1} hydrochloric acid. After a certain amount of flocculant was added, the mixture was stirred at the speed of 200–450 rpm for 1.5–4 min to mix the flocculants and suspended particles, then at 30–80 rpm for 8–13 min to grow the flocs, and finally settled for 30 min. After flocculation, the supernatant turbidity 1 cm below the water surface was measured by a turbidity indicator (WGZ-4000B, Xinrui, China). The turbidity removal efficiency was adopted to evaluate the flocculation performance of the flocculants.

2.7. Sterilization experiment

LB broth powder of 25 g was dissolved in 1 L of deionized water, and its pH value was adjusted to 7 by adding 0.1 mol L^{-1} sodium hydroxide solution. The subsequent experiments were performed under gnotobasis. The culture solution and glasswares were autoclaved at 121°C for 30 min. *E. coli* was inoculated in a 250 mL flask containing an appropriate amount of LB culture solution for 24 h. The culture solution was then poured into centrifuge tubes and centrifuged at a speed of 3,000 rpm for 5 min to separate *E. coli* and the culture medium. After the upper culture medium was removed, a certain amount of *E. coli* sediment was obtained and dispersed in water to obtain a concentration of approximately 1×10^7 CFU mL^{-1}. After the flocculant was added, the same procedure as the flocculation experiment was performed. The optical density at 600 nm (OD600) of the supernatant before and after the flocculation was measured at 600 nm wavelength by a UV spectrophotometer (UV-4800, UNICO, China), and the sterilization mechanism

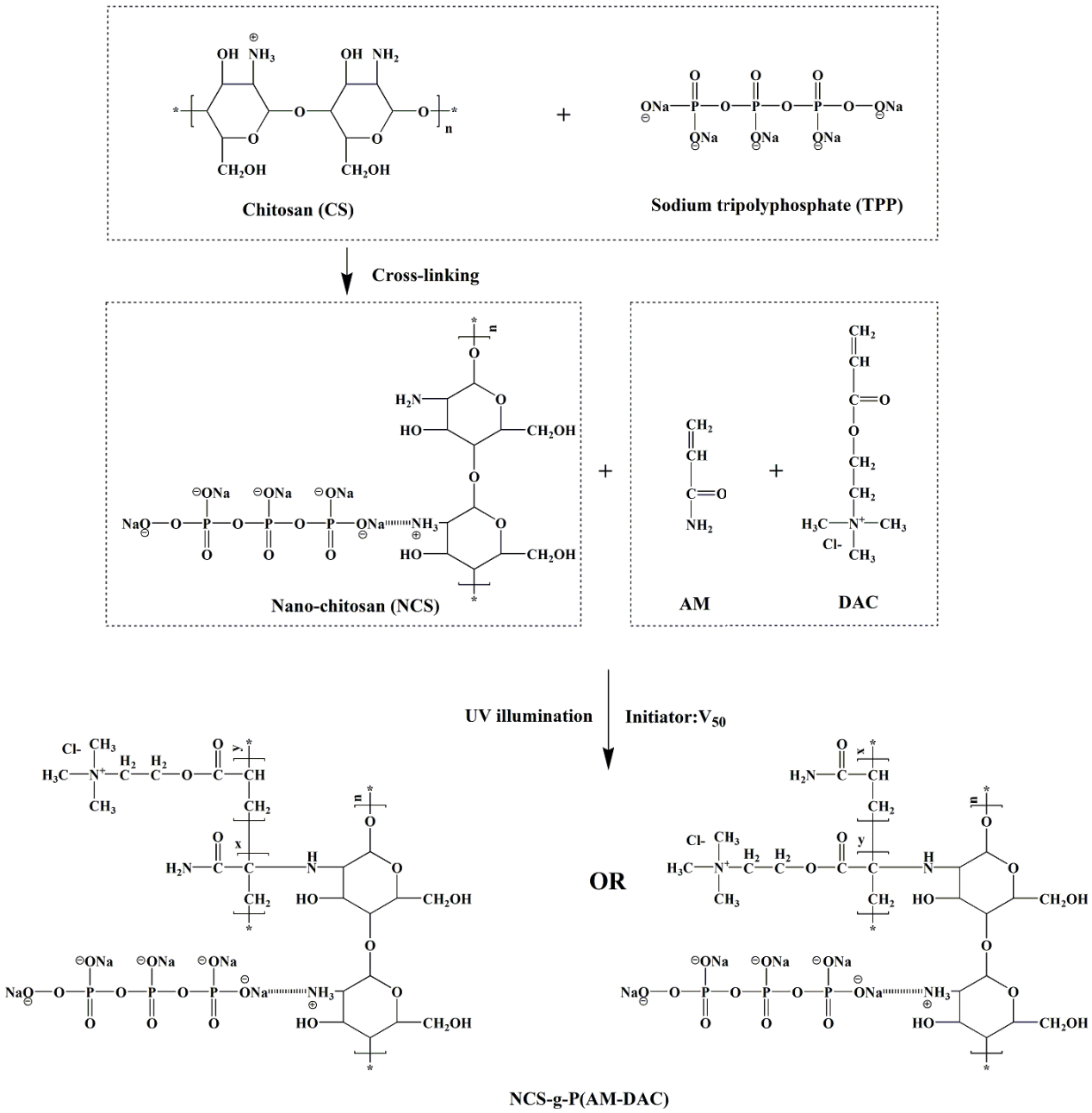

Fig. 1. Possible schematic diagram of graft copolymerization.

of NCS-g-P(AM-DAC) in the reaction was further studied by 3D-EEM (LS-55, PerkinElmer, USA).

3. Results and discussion

3.1. Synthesis conditions optimization

The intrinsic viscosity influences flocculants efficiency [37]. To obtain the flocculants with high intrinsic viscosity, the effects of monomer mass ratio (CS:TPP, AM:CS, DAC:CS), stirring time, ultrasonic time, initiator dosage, and UV illumination time on the intrinsic viscosity was studied. From the experiment data in Fig. 2, the optimum values of monomer mass ratio (CS:TPP, AM:CS, DAC:CS) was 5:1, 9:1, 3:1, whereas stirring time, ultrasonic time, initiator dosage, and UV illumination time were 25 min, 6 min, 0.8% by mass of the monomer, and 2 h, respectively.

3.2. Charaterization of flocculants

The FT-IR spectra of CS, NCS, chitosan-graft-poly(acrylamide and acryloyloxyethyltrimethyl ammonium chloride (CS-g-P(AM-DAC)), and NCS-g-P(AM-DAC) are shown in Fig. 3. The bands at 3,344; 1,620; and 1,083 cm^{-1} were attributed to the stretching vibration of O–H, N–H, and C–O–C groups of CS respectively [31,38]. In Fig. 3b a new

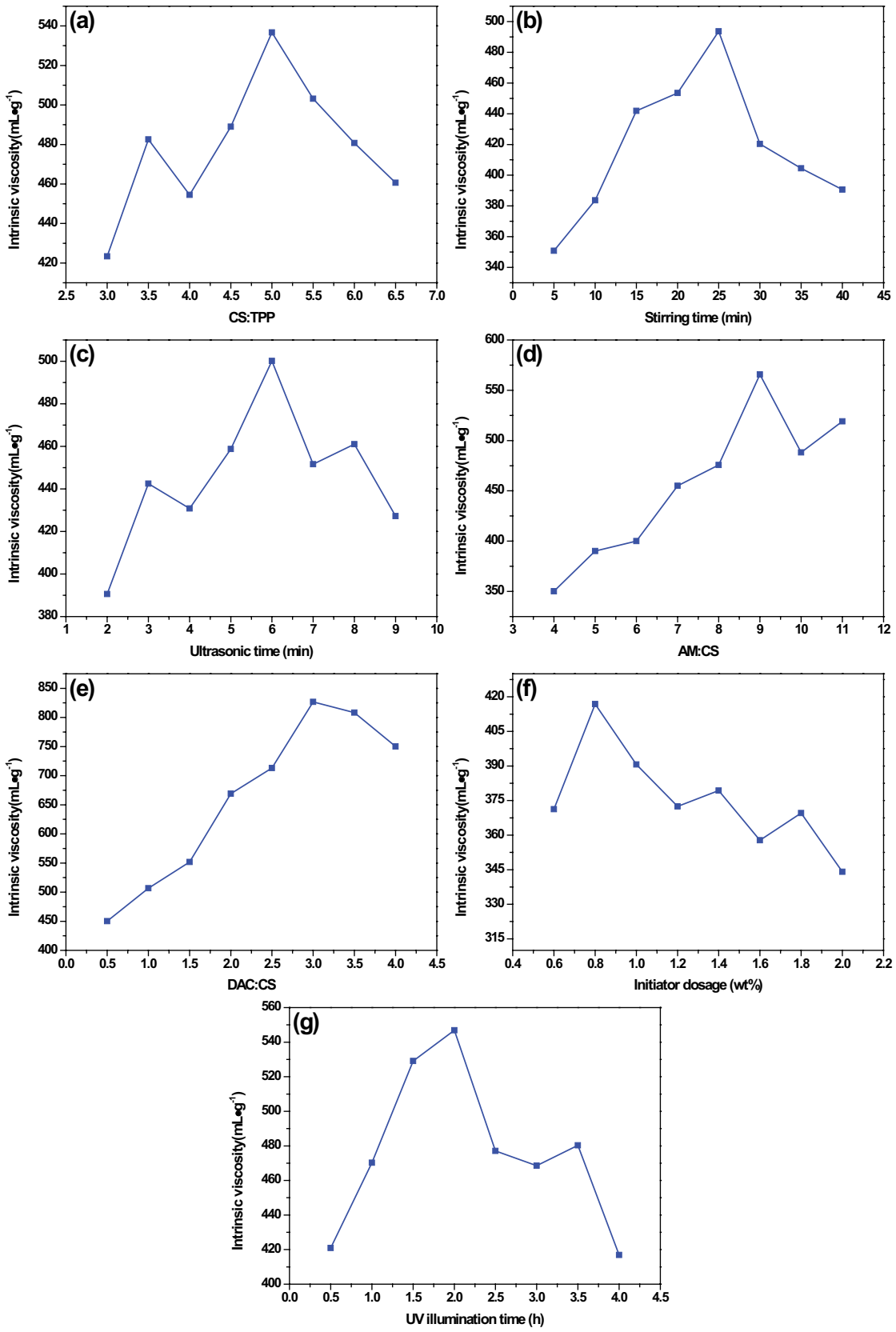

Fig. 2. Effect of (a) CS:TPP, (b) stirring time, (c) ultrasonic time, (d) AM:CS, (e) DAC:CS, (f) initiator dosage, and (g) UV illumination time on intrinsic viscosity.

absorption peak appeared at approximately 1,270 cm^{-1} and corresponded to P=O stretching vibration, thus confirming the successful preparation of NCS through the ionic gelation and the electronic interaction between ammonium ions and phosphoric groups [39]. As illustrated in Figs. 3c and 3d, the peaks at 3,190; 1,666; and 1,606 cm^{-1} were attributed to the N–H, C=O, and C=C stretching on PAM, respectively [17]. The peaks at 1,419 and 904 cm^{-1} were attributed to the $–CH_2–$ in $–CH_2–N^+$ group and $–N^+–(CH_3)_3$ to the stretching on the DAC [40,41]. Besides, the peaks of the characteristic functional groups mentioned above appeared on the spectra of NCS-g-P(AM-DAC) in Fig. 3d. The results of FT-IR spectral analysis confirmed that PAM and DAC have been successfully grafted on NCS.

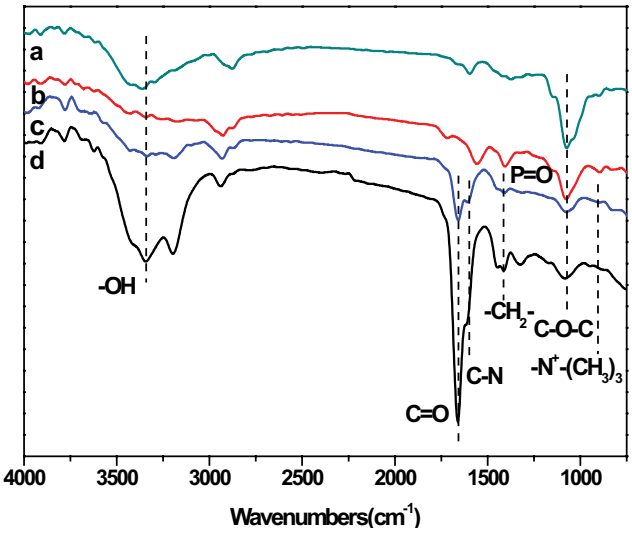

Fig. 3. FT-IR of (a) CS, (b) NCS, (c) CS-g-P(AM-DAC), and (d) NCS-g-P(AM-DAC).

The SEM analysis of CS, NCS, CS-g-P(AM-DAC), and NCS-g-P(AM-DAC) in Fig. 4 revealed that NCS-g-P(AM-DAC) presented a profound morphological change. Fig. 4b shows that compared with CS in Fig. 4a, the surface of NCS changed greatly after grafting and the surface was relatively rough with a few tiny holes. As shown in Fig. 4d, after AM and DAC were grafted onto the NCS, its morphology was quite different from that of other flocculants due to the flocculant surface activation and the generation of free radicals, which destroyed the primitive ordered crystal structure of NCS and increased the surface roughness. The surface of NCS had changed from being merely rough to having course and irregular porous and the pore size had notably improved. This change positively contributed to the flocculation because profuse holes were favorable for the improving of flocculation and water solubility [31,34,42].

The details of weight loss and corresponding temperature were all listed in Table 1. According to the TG curves of CS and NCS in Figs. 5a and b, three stages of

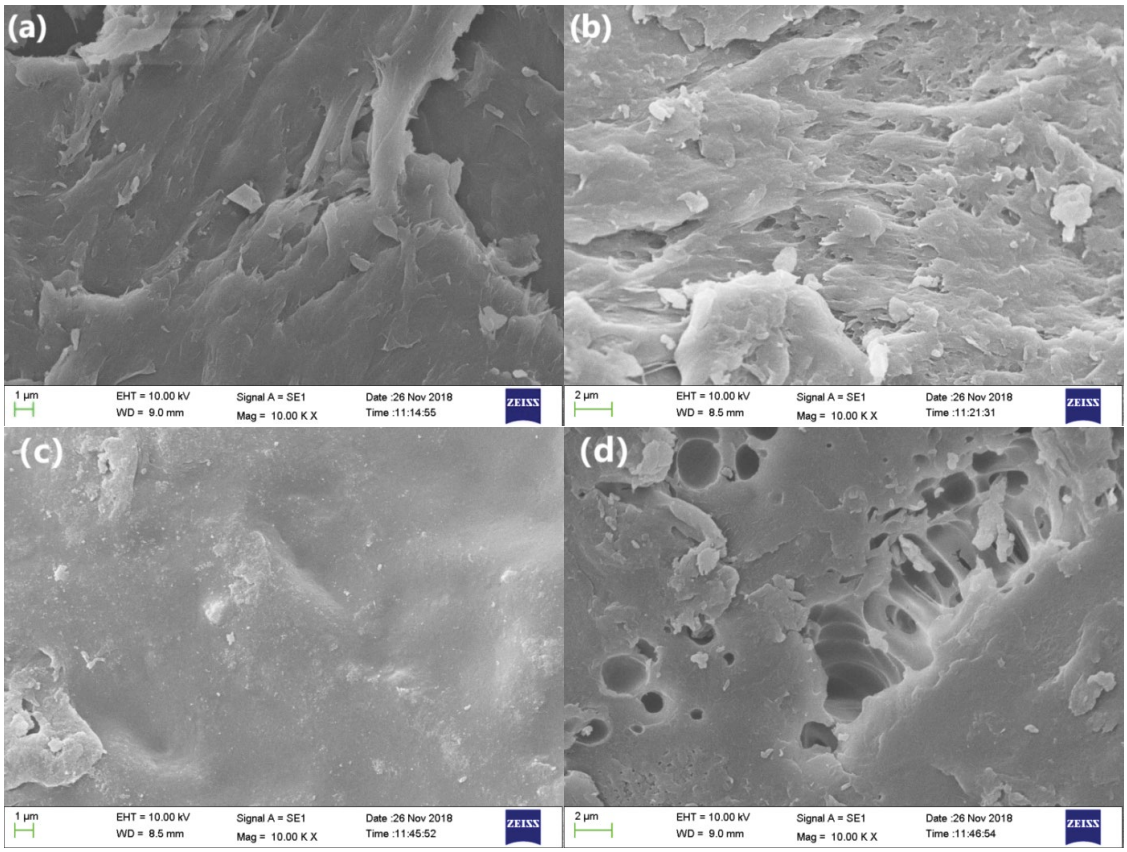

Fig. 4. SEM of (a) CS, (b) NCS, (c) CS-g-P(AM-DAC), and (d) NCS-g-P(AM-DAC).

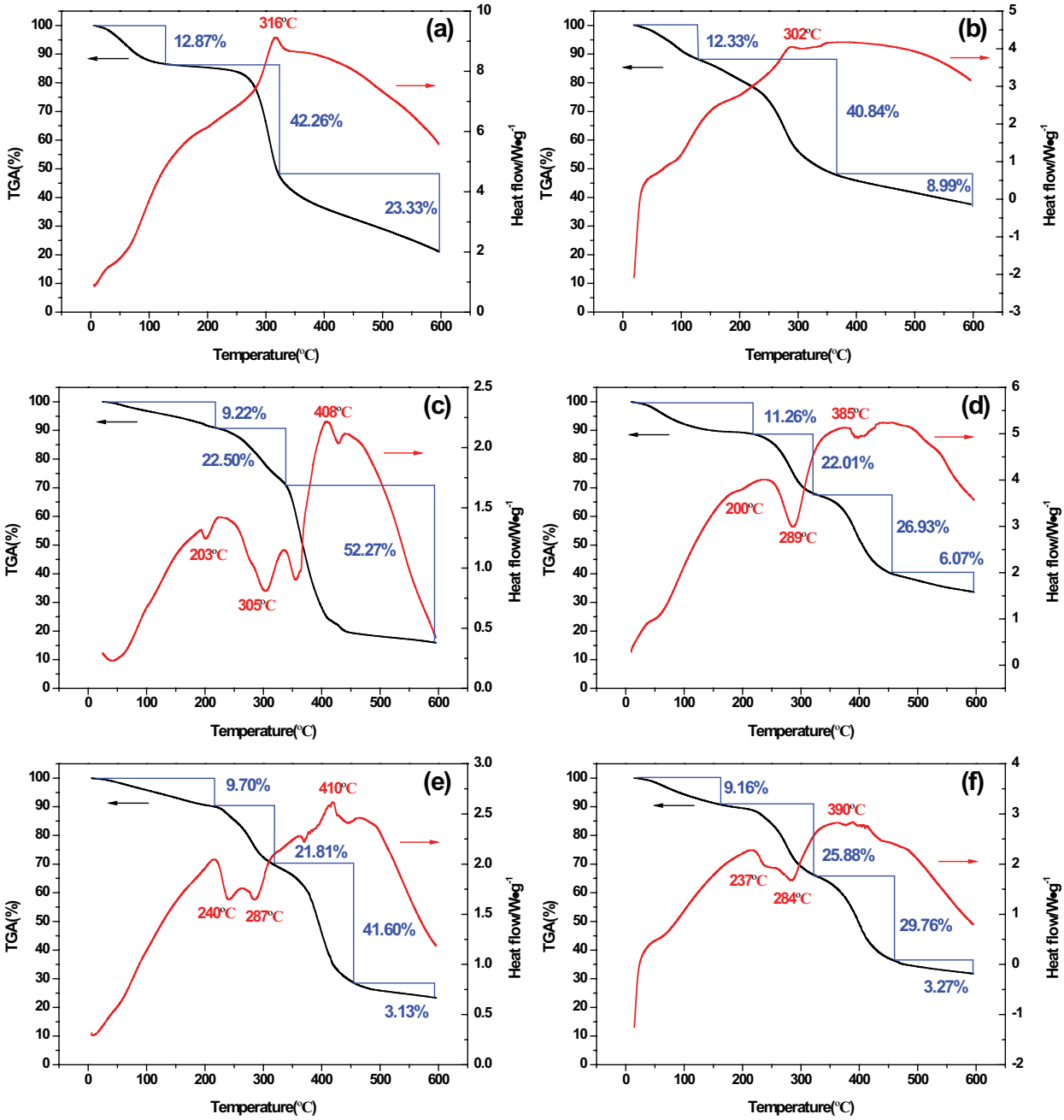

Fig. 5. TG/DSC of (a) CS, (b) NCS, (c) PAM, (d) NCS-g-PAM, (e) CS-g-P(AM-DAC), and (f) NCS-g-P(AM-DAC).

weight loss were observed. For CS, the weight loss of the first stage occurred at 13.03°C–121.06°C, whereas it was 26.97°C–137.87°C for NCS. In this range, the weight loss was 12.87% and 12.33%, respectively. The first weight loss was due to the sample moisture adsorption, which was removed under heat and dry conditions [5,33]. The weight loss temperature range of the second stage was 121.06°C–334.06°C for CS and 137.87°C–385.41°C for NCS, in which the weight loss of the two reached 42.26% and 40.84%, respectively. The main reason was that the functional groups, such as –OH, on the CS backbone were decomposed [43]. The decomposition of the third stage occurred after 334.06°C and 385.41°C respectively. For CS and NCS, the weight loss was 23.33% and 8.99%, respectively, mainly attributed to the decomposition of the CS backbone [5,34,38]. In comparison, NCS was more thermal stable than CS. From Fig. 5c PAM exhibits three stages of weight loss. The first stage occurred at 29.92°C–222.84°C, wherein the weight loss was 9.22% due to the removal of moisture adsorption. The second stage occurred at 222.84°C–345.36°C, wherein the PAM weight loss was 22.5%. In this stage, the weight loss was mainly attributed to the decomposition of the amide groups [5,34]. The third stage occurred after 345.36°C, which was the decomposition of the PAM molecular chain.

Table 1
TGA details

Sample	Stage one (°C)	WL (%)	Stage two (°C)	WL (%)	Stage three (°C)	WL (%)	Stage four (°C)	WL (%)
CS	13.03	12.87	121.06	42.26	334.06	23.33	–	–
NCS	26.97	12.33	137.87	40.84	385.41	8.99	–	–
PAM	29.92	9.22	222.84	22.5	345.36	52.27	–	–
NCS-g-PAM	20.87	11.26	226.07	22.01	341.14	26.93	460.68	6.07
CS-g-P(AM-DAC)	24.32	9.7	219.89	21.81	333.84	41.6	482.71	3.13
NCS-g-P(AM-DAC)	23.18	9.16	164.11	25.88	337.49	29.76	476.3	3.27

WL: weight loss.

From Figs. 5d–f, NCS-graft-polyacrylamide (NCS-g-PAM), CS-g-P(AM-DAC), and NCS-g-P(AM-DAC) all showed similar thermal decomposition trends and thermal decomposition characteristics as CS and PAM. For NCS-g-P(AM-DAC), the first stage weight loss was 9.16%, and the second stage weight loss was 25.88%. In addition to the decomposition of CS and PAM functional groups, NCS-g-P(AM-DAC) also included methylation on the quaternary ammonium salt [5,33]. So NCS-g-P(AM-DAC) lost more weight than NCS-g-PAM in this stage. The third stage was the decomposition of the molecule chain of the polymer, wherein the weight loss was 29.76%. Then the TG curve tended to be gentle, and the final residual weight was approximately 31.77%. In addition, the endothermic peaks and the exothermic peaks in the DSC curve of PAM, NCS-g-PAM, and CS-g-P(AM-DAC) could be also discovered in the NCS-g-P(AM-DAC). Moreover, all the nano-modified flocculants exhibited much better stability and higher residual weight than others, confirming the existence of nanoparticles [44]. TGA result confirmed that the grafting of PAM and DAC was successful from the other angle, and the NCS-g-P(AM-DAC) synthesized by UV-initiation graft copolymerization was stable at room temperature and did not decompose.

As shown in Figs. 6a and 6b, the size distribution of chitosan-graft-polyacrylamide (CS-g-PAM) was within the range of 4.19–15.69 nm, whereas that of CS-g-P(AM-DAC) was in the range of 11.67–21.04 nm. After the ion cross-linking, the particle size was slightly enlarged. Fig. 6c shows that the size distribution of NCS-g-P(AM-DAC) with an average diameter of 43.82–122.42 nm in narrow size distribution (Polymer dispersity index = 0.650). In general, NCS was easy to aggregate because of Van der Waals forces. However, according to the DLVO theory, this effect can be reduced by electrostatic repulsion. Thus, the electrostatic repulsion was enhanced due to grafting of DAC and the aggregation possibility was reduced [45]. In addition, the narrow size proved its stability as presented in the curve. As reported, the particle size of NCS mainly depended on the ratio and concentration of CS and TPP. Therefore, the ratio and concentration of CS and TPP used in this study were suitable [46].

3.3. Flocculation performance

The flocculation performance of CS-g-PAM, CS-g-P(AM-DAC), and NCS-g-P(AM-DAC) under different dosages and pH conditions was investigated. Initial pH = 7.0 ± 0.1 was kept constant in the dosage experiment. From Fig. 7 the removal efficiency of all flocculants increased with the dosage increased and the highest turbidity removal efficiency

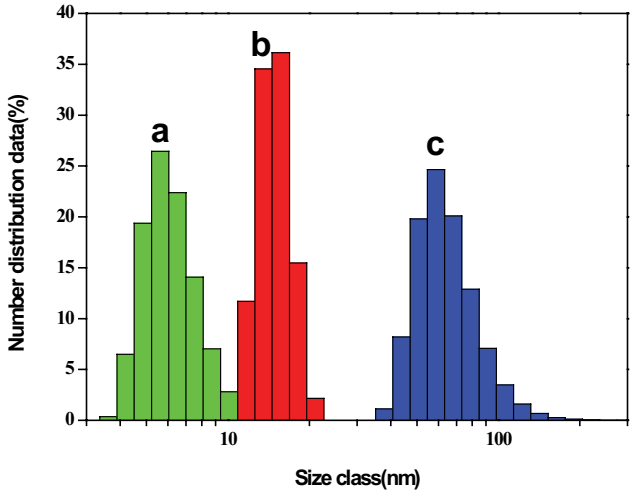

Fig. 6. Particle size distribution of (a) CS-g-PAM, (b) CS-g-P(AM-DAC), and (c) NCS-g-P(AM-DAC).

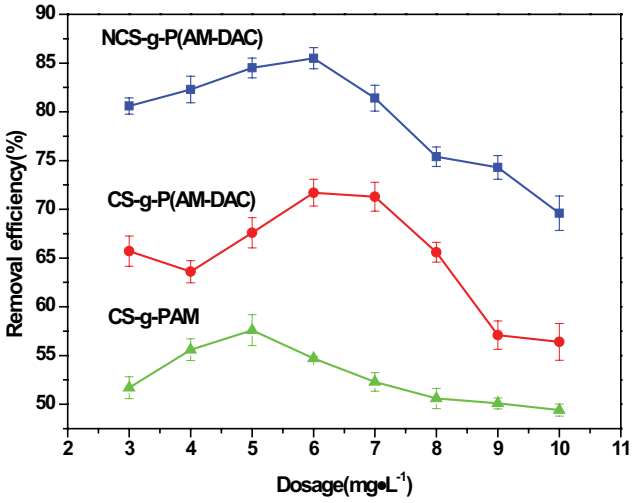

Fig. 7. Effect of dosage on turbidity removal efficiency of CS-g-PAM, CS-g-P(AM-DAC), and NCS-g-P(AM-DAC).

of CS-g-PAM, CS-g-P(AM-DAC) and NCS-g-P(AM-DAC) reached 57.6% at the dosage of 5 mg L^{-1}, 71.1% at the dosage of 6 mg L^{-1}, 85.5% at the dosage of 6 mg L^{-1}, respectively. This result indicated that a positive charge on the surface of the flocculant was insufficient to neutralize the negative charge on the surface of the kaolin at the beginning. With the dosage increasing continuously, the electrical neutralization played a major role. But when the dosage exceeded a certain value, the turbidity removal efficiency gradually decreased. The floc particles were off-stabilized and resuspended in the supernatant because the flocculation system underwent charge reversal [34]. With the introduction of DAC, the removal efficiency of CS-g-P(AM-DAC) was improved greatly compared that of CS-g-PAM due to the enhancement of the positive charge. In addition, when the CS in the copolymer was replaced by NCS, the turbidity removal efficiency could be improved by 20% to 25%. This result indicated that the flocculation performance of NCS-g-P(AM-DAC) was enhanced due to the morphology change and the positive charge long-chain [31]. In summary, NCS-g-P(AM-DAC) showed better flocculation performance than the other two flocculants.

From Fig. 8 NCS-g-P(AM-DAC) exhibits higher and more stable removal efficiency than CS-g-P(AM-DAC) at kaolin suspensions under various pH levels. The turbidity removal rate of NCS-g-P(AM-DAC) first increased and reached 89.2% at pH = 6, whereas the removal efficiency of CS-g-PAM and CS-g-P(AM-DAC) all increased at the beginning. In addition, optimum efficiency was 55.6% at pH = 7 and 66.4% at pH = 5, respectively. All flocculants also exhibited the same trend that the turbidity removal efficiency increased first and then decreased with the increase of pH. Besides, the efficiency was relatively high under acidic and neutral conditions but deteriorated under alkaline conditions. This phenomenon occurred because, under acidic or neutral conditions, the flocculant was abundant in positive charge and thus exhibited an excellent ability of charge neutralization, which was favorable to charge for the negatively charged kaolin suspension particles. In addition, the electrostatic repulsion action enhanced greatly because of the grafting of PAM and DAC onto the skeleton of NCS. As a result, the molecular chain of flocculants tended to be stretched, which was favorable for the bridging action. Meanwhile, the effects mentioned above were reversed under alkaline conditions. The acidic condition was appropriate for NCS-g-P(AM-DAC) flocculation. Compared with that of NCS-g-P(AM-DAC), the flocculation effect of CS-g-PAM and CS-g-P(AM-DAC) under acidic conditions was significantly weaker and deteriorated, because CS was easily dissolved and hydrolyzed under acidic conditions, thus causing the flocculants to degrade.

Given that the charge properties of flocculants greatly influenced the flocculation effect and flocculation performance, the zeta potential values of the flocculant, the kaolin suspension, and *E. coli* suspension were measured. Their pH dependence is shown in Fig. 9. The zeta potential for NCS-g-P(AM-DAC) decreased with an increase in pH. A positive charge was seen at pH ≤ 8.1, whereas the zeta potential became negative at pH > 8.1. Besides, kaolin suspension showed a negative charge within the pH range, whereas *E. coli* suspension contained a negative surface charge when pH > 3.2. NCS-g-P(AM-DAC) revealed an opposite electrical property with the tested synthetic effluents merely in the pH range of 3.2 to 8.1, in which NCS-g-P(AM-DAC) prominently exhibited a charge neutralization effect [19,47].

3.4. Sterilization performance

In this section, the OD600 removal experiment was employed to investigate the sterilization performance of flocculants because the OD600 value had a linear relationship with the number of bacteria. pH = 6 of the *E. coli* suspension was kept unchanged for sterilization experiments. The effect of different dosages of PAM, CS-g-PAM, CS-g-P(AM-DAC), and NCS-g-P(AM-DAC) on the OD600 removal efficiency was investigated. The results are shown in Fig. 10. Except for PAM and CS-g-PAM, the other two flocculants containing quaternary ammonium salts showed removal effects of

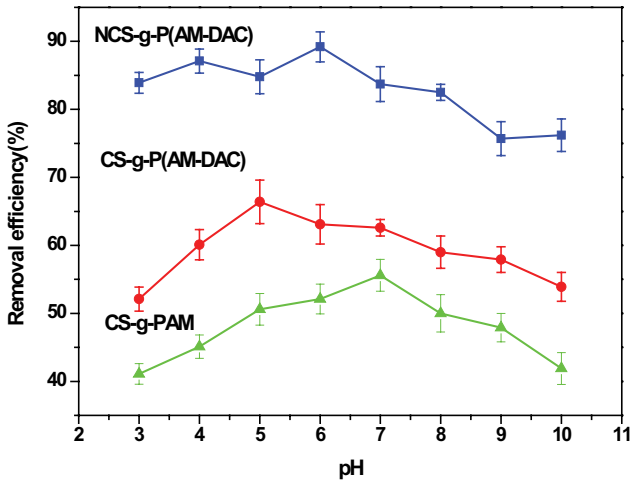

Fig. 8. Effect of pH on the turbidity removal efficiency of CS-g-PAM, CS-g-P(AM-DAC), and NCS-g-P(AM-DAC) (dosage: 5 mg·L^{-1}).

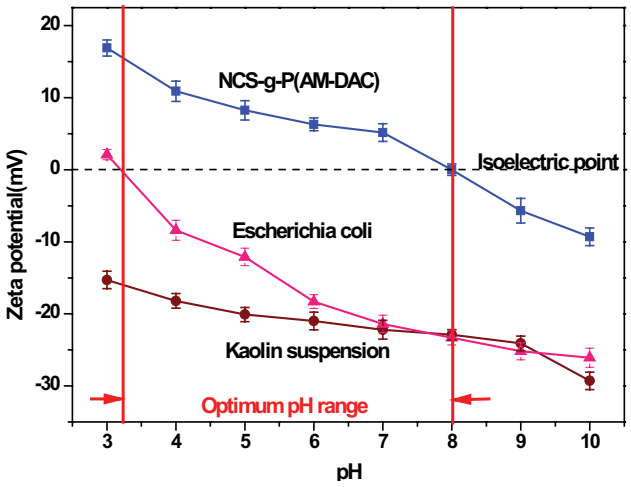

Fig. 9. Zeta potential vs. pH profiles of NCS-g-P(AM-DAC), kaolin suspension, and *Escherchia coli* suspension.

E. coli. They reached the highest efficiencies of 2.18%, 7.10%, 73.53%, and 92.96%, respectively. The comparison between PAM and CS-g-PAM revealed that the sterilization property of flocculant was enhanced slightly due to the amino groups on the CS skeleton. With the introduction of DAC, the removal rate of CS-g-P(AM-DAC) was enhanced obviously, confirming the improvement of sterilization property was mainly assigned to the quaternary ammonium[5]. Besides, the removal efficiency of OD600 by NCS-g-P(AM-DAC) was prominent and the corresponding optimum dosage was lower compared with CS-g-P(AM-DAC). It can be speculated that the molecular chains could be stretched by charge repulsion and stretched molecular chain. The nanoparticles of the special structure on the molecular chain could extensively and effectively capture bacteria. Therefore, NCS-g-P(AM-DAC) could flocculate simultaneously with the adsorption neutralization and bridging. From the results of flocculation experiments and sterilization tests, NCS-g-P(AM-DAC) exhibited excellent effects during flocculation and sterilization.

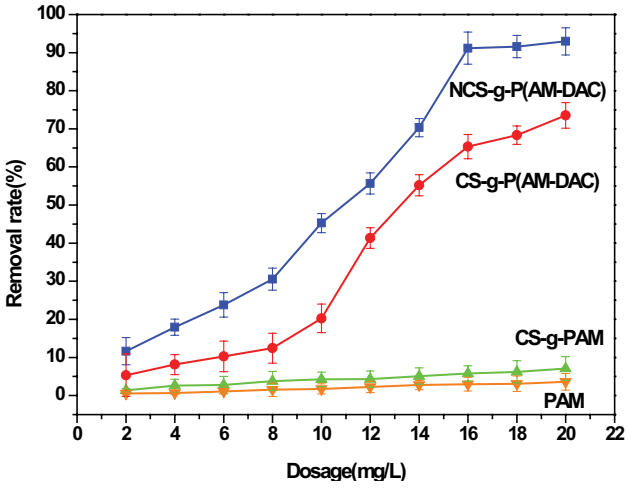

Fig. 10. Effect of dosage of CS-g-PAM, CS-g-P(AM-DAC), and NCS-g-P(AM-DAC) on the flocculation of *Escherichia coli* suspension.

3.5. Sterilization mechanism

The sterilization mechanism of NCS-g-P(AM-DAC) in the flocculation was further analyzed with the aid of 3D-EEM. Given that the aromatic compound has a conjugated unsaturated system, it can fluoresce under UV light irradiation. Therefore, whether the aromatic protein in *E. coli* was released via the fluorescence signal of the local region of the aromatic protein and the signal intensity in the fluorescence spectrum must be determined [48]. The pH = 6 of *E. coli* suspension was maintained, and the supernatant of untreated *E. coli* suspension, treated by the various dosages of the NCS-g-P(AM-DAC) were subjected to 3D-EEM

3D-EEM revealed that a fluorescent signal of aromatic protein appeared at the region I of the spectrum (emission wavelength: 250–280 nm, excitation wavelength: 280–370 nm). From Fig. 11b the fluorescent signal was weak at a low dosage. This value was almost unchanged similar to that of the untreated sample in Fig. 11a. The signal in this part may be due to a small amount of protein derived from

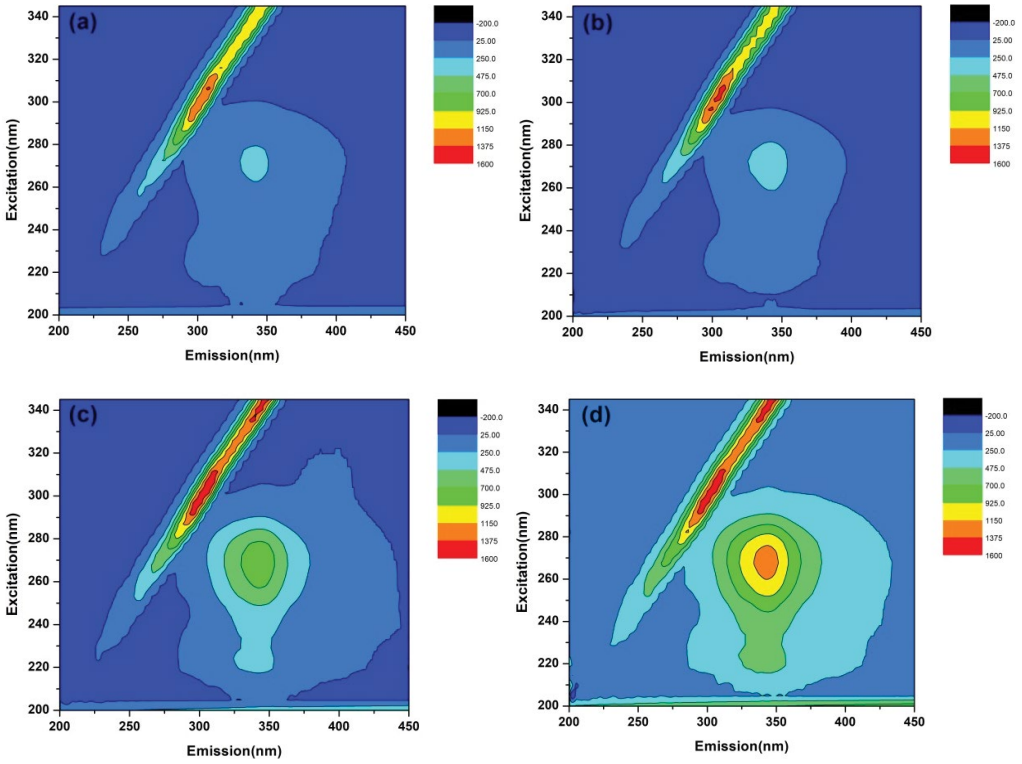

Fig. 11. 3D-EEM spectra of supernatants of *Escherichia coli* suspension treated by different dosage of NCS-g-P(AM-DAC). (a) 0 mg·L^{-1}, (b) 2 mg·L^{-1}, (c) 5 mg·L^{-1}, and (d) 10 mg·L^{-1}.

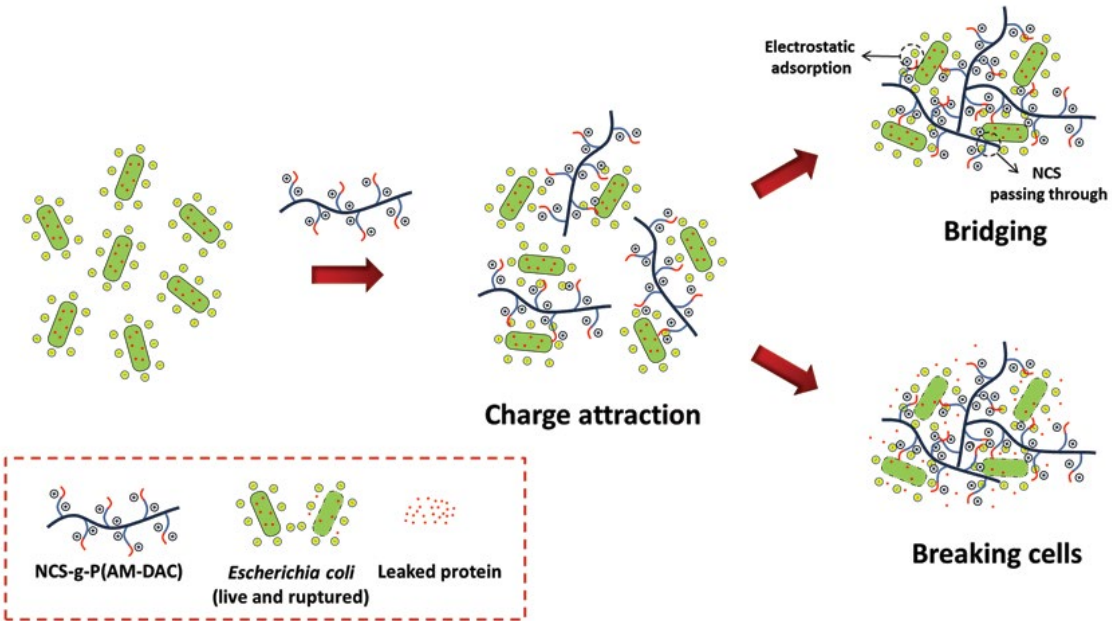

Fig. 12. Schematic diagram of sterilization mechanism.

the metabolism of *E. coli* cells during the treatment. With the increase in dosage, the fluorescence signal was continuously enhanced in Figs. 11c–d. This result indicated that a large amount of aromatic protein appeared in the solution. It was speculated that several cell membranes of *E. coli* were severely impaired and damaged, and a large amount of aromatic protein was released and leaked [49]. The results showed that NCS-g-P(AM-DAC) could destroy the cellular structure and at this time NCS-g-P(AM-DAC) played a bactericidal role.

In summary, the sterilization mechanism was pictured and shown in Fig. 12. The NCS-g-P(AM-DAC) with strong electrostatic adsorption could be adsorbed on the negatively charged cell cytoderm at the beginning [50], and then the *E. coli* cells in the solution destabilized when the repulsion decreased. This condition was favorable for the aggregation and formation of large bacterial flocs under charge neutralization and bridging. After an excess amount of NCS-g-P(AM-DAC) was added, the quaternary ammonium groups and some amino groups on the molecular chain were adsorbed on the surface of *E. coli* due to electrostatic attraction and hydrogen bonding. Thus, the ion concentration on the surface of the cell membrane suddenly increased, resulting in the unbalance of the osmotic pressure on both sides of the cell membrane [34,51]. The unbalance rendered the cell membrane to lose its permeability, leading to cell destabilization and causing the death and rupture of cells. In addition, nanoparticles could relatively easily pass through the cell membrane, enter into the bacteria and combine with the proteins in the cell-matrix. The normal metabolism of bacteria was then hindered, leading to bacteria death [52].

4. Conclusions

In this study, a novel flocculant with sterilization and flocculation functions was synthesized by grafting AM and DAC onto NCS through UV-initiation. The material was successfully fabricated and confirmed by characterization analytical results. The optimum synthesis conditions for the intrinsic viscosity of NCS-g-P(AM-DAC) were optimized. The flocculation experiment results proved that NCS-g-P(AM-DAC) exhibited excellent and stable flocculation performance under different pH levels because of the nanoparticle's grafted long-chain and high positive charge. On the basis of the sterilization experiments, its sterilization performance was strengthened due to the grafting of quaternary ammonium salts. In addition, 3D-EEM confirmed that NCS-g-P(AM-DAC) was not just antibacterial, but in fact bactericidal. During the water treatment process, the simultaneous flocculation and sterilization in the flocculation process can reduce the amount of the bactericide that is added in the subsequent process to avoid the risk of secondary contamination by the generated disinfection by-products. This finding is important for the actual water treatment project and can enrich the technology and promote the development of the flocculation.

Acknowledgments

The work was supported by the National Natural Science Foundation of China (Project No. 21677020), Sichuan education department project (Project No. 18ZB0463), Innovative experiment projects of Sichuan Agricultural University (Project No. 201710626058), and Research interest development program of Sichuan Agricultural University (Project No. 2019692). Kind suggestions from the anonymous reviewers are greatly acknowledged by authors.

References

[1] J.Y. Ma, J. Shi, H.C. Ding, G.C. Zhu, K. Fu, X. Fu, Synthesis of cationic polyacrylamide by low-pressure UV initiation for turbidity water flocculation, Chem. Eng. J., 312 (2017) 20–29.

[2] Y.J. Sun, K.J. Shah, W.Q. Sun, H.L. Zheng, Performance evaluation of chitosan-based flocculants with good pH resistance and high heavy metals removal capacity, Sep. Purif. Technol., 215 (2019) 208–216.
[3] X. Huang, Y. Zhao, B.Y. Gao, S.L. Sun, Y. Wang, Q. Li, Q.Y. Yue, Polyacrylamide as coagulant aid with polytitanium sulfate in humic acid-kaolin water treatment: effect of dosage and dose method, J. Taiwan Inst. Chem. Eng., 64 (2016) 173–179.
[4] S.Y. Jia, Z. Yang, W.B. Yang, T.T. Zhang, S.P. Zhang, X.Z. Yang, Y.Y. Dong, J.Q. Wu, Y.P. Wang, Removal of Cu(II) and tetracycline using an aromatic rings-functionalized chitosan-based flocculant: enhanced interaction between the flocculant and the antibiotic, Chem. Eng. J., 283 (2016) 495–503.
[5] M. Wang, L. Feng, X.W. Fan, D.M. Li, W.G. Qu, S.X. Jiang, S.X. Li, Fabrication of bifunctional chitosan-based flocculants: characterization, assessment of flocculation, and sterilization performance, Materials, 11 (2018) 2009.
[6] C.L. Zhao, H.L. Zheng, Y.J. Sun, S.X. Zhang, J.J. Liang, Y.Z. Liu, Y.Y. An, Evaluation of a novel dextran-based flocculant on treatment of dye wastewater: effect of kaolin particles, Sci. Total Environ., 640–641 (2018) 243–254.
[7] J.J. Xun, T. Lou, J.S. Xing, W.X. Zhang, Q. Xu, J. Peng, X.J. Wang, Synthesis of a starch–acrylic acid–chitosan copolymer as flocculant for dye removal, J. Appl. Polym. Sci., 136 (2019) 47437.
[8] M. Huang, Y. Wang, J. Cai, J.F. Bai, H. Yang, A.M. Li, Preparation of dual-function starch-based flocculants for the simultaneous removal of turbidity and inhibition of *Escherichia coli* in water, Water Res., 98 (2016) 128–137.
[9] S.M. Ahsan, M. Thomas, K.K. Reddy, S.G. Sooraparaju, A. Asthana, I. Bhatnagar, Chitosan as biomaterial in drug delivery and tissue engineering, Int. J. Biol. Macromol., 110 (2018) 97–109.
[10] I.M. Minisy, N.A. Salahuddin, M.M. Ayad, Chitosan/polyaniline hybrid for the removal of cationic and anionic dyes from aqueous solutions, J. Appl. Polym. Sci., 136 (2019) 47056.
[11] J.H. Wang, L. Wang, H.J. Yu, Zain-ul-Abdin, Y.S. Chen, Q. Chen, W.D. Zhou, H.T. Zhang, X. Chen, Recent progress on synthesis, property and application of modified chitosan: an overview, Int. J. Biol. Macromol., 88 (2016) 333–344.
[12] C.Q. Zhu, F.Q. Liu, Y.H. Zhang, M.M. Wei, X.P. Zhang, C. Ling, A.M. Li, Nitrogen-doped chitosan-Fe(III) composite as a dual-functional material for synergistically enhanced co-removal of Cu(II) and Cr(VI) based on adsorption and redox, Chem. Eng. J., 306 (2016) 579–587.
[13] Z. Yang, J.-R. Degorce-Dumas, H. Yang, E. Guibal, A.M. Li, R.S. Cheng, Flocculation of *Escherichia coli* using a quaternary ammonium salt grafted carboxymethyl chitosan flocculant, Environ. Sci. Technol., 48 (2014) 6867–6873.
[14] B. Zakaria Djibrine, H. Zheng, M. Wang, S. Liu, X.M. Tang, S. Khan, A.N. Jimenéz, L. Feng, An effective flocculation method to the kaolin wastewater treatment by a cationic polyacrylamide (CPAM): preparation, characterization, and flocculation performance, Int. J. Polym. Sci., 2018 (2018) 1–12.
[15] P.R. Suresha, M.V. Badiger, Flocculation of kaolin from aqueous suspension using low dosages of acrylamide-based cationic flocculants, J. Appl. Polym. Sci., 136 (2018) 47286.
[16] M. Said, Y. Atassi, M. Tally, H. Khatib, Environmentally friendly chitosan-g-poly(acrylic acid-*co*-acrylamide)/ground basalt superabsorbent composite for agricultural applications, J. Polym. Environ., 26 (2018) 3937–3948.
[17] T. Lou, X.J. Wang, G.J. Song, G.P. Cui, Synthesis and flocculation performance of a chitosan-acrylamide-fulvic acid ternary copolymer, Carbohydr. Polym., 170 (2017) 182–189.
[18] A.G. Ibrahim, A.S. Saleh, E.M. Elsharma, E. Metwally, T. Siyam, Gamma radiation-induced preparation of poly(1-vinyl-2-pyrrolidone-co-sodium acrylate) for effective removal of Co(II), Ni(II), and Cu(II), Polym. Bull., 76 (2019) 303–322.
[19] C.F. Zhao, S. Shao, Y.Y. Zhou, Y.H. Yang, Y. Shao, L.P. Zhang, Y. Zhou, L. Xie, L. Luo, Optimization of flocculation conditions for soluble cadmium removal using the composite flocculant of green anion polyacrylamide and PAC by response surface methodology, Sci. Total Environ., 645 (2018) 267–276.
[20] J.M. Klein, V.S. de Lima, J.M.C. da Feira, M. Camassola, R.N. Brandalise, M.M. de Camargo Forte, Preparation of cashew gum-based flocculants by microwave- and ultrasound-assisted methods, Int. J. Biol. Macromol., 107 (2018) 1550–1558.
[21] J.Y. Ma, J. Shi, L. Ding, H. Zhang, S. Zhou, Q.J. Wang, X. Fu, L. Jiang, K. Fu, Removal of emulsified oil from water using hydrophobic modified cationic polyacrylamide flocculants synthesized from low-pressure UV initiation, Sep. Purif. Technol., 197 (2018) 407–417.
[22] L. Chen, H. Zhu, Y.J. Sun, P.-C. Chiang, W.Q. Sun, Y.H. Xu, H.L. Zheng, K.J. Shah, Characterization and sludge dewatering performance evaluation of the photo-initiated cationic flocculant PDD, J. Taiwan Inst. Chem. Eng., 93 (2018) 253–262.
[23] B. Liu, H. Zheng, Y. Wang, X. Chen, C. Zhao, Y. An, X. Tang, A novel carboxyl-rich chitosan-based polymer and its application for clay flocculation and cationic dye removal, Sci. Total Environ., 640–641 (2018) 107–115.
[24] H.-L. Fan, S.-F. Zhou, W.-Z. Jiao, G.-S. Qi, Y.-Z. Liu, Removal of heavy metal ions by magnetic chitosan nanoparticles prepared continuously via high-gravity reactive precipitation method, Carbohydr. Polym., 174 (2017) 1192–1200.
[25] F. Polesel, J. Farkas, M. Kjos, P.A. Carvalho, X. Flores-Alsina, K.V. Gernaey, S.F. Hansen, B.G. Plósz, A.M. Booth, Occurrence, characterisation and fate of (nano)particulate Ti and Ag in two Norwegian wastewater treatment plants, Water Res., 141 (2018) 19–31.
[26] J.Y. Ma, X. Fu, L. Jiang, G.C. Zhu, J. Shi, Magnetic flocculants synthesized by Fe_3O_4 coated with cationic polyacrylamide for high turbid water flocculation, Environ. Sci. Pollut. Res., 25 (2018) 25955–25966.
[27] J. Huang, G. Huang, C. An, Y. He, Y. Yao, P. Zhang, J. Shen, Performance of ceramic disk filter coated with nano ZnO for removing *Escherichia coli* from water in small rural and remote communities of developing regions, Environ. Pollut., 238 (2018) 52–62.
[28] K.-Y. Chen, S.-Y. Zeng, Fabrication of quaternized chitosan nanoparticles using tripolyphosphate/genipin dual cross-linkers as a protein delivery system, Polymers-Basel, 10 (2018) 1226.
[29] E.M.A. Hejjaji, A.M. Smith, G.A. Morris, Evaluation of the mucoadhesive properties of chitosan nanoparticles prepared using different chitosan to tripolyphosphate (CS:TPP) ratios, Int. J. Biol. Macromol., 120 (2018) 1610–1617.
[30] P.L. Kashyap, X. Xiang, P. Heiden, Chitosan nanoparticle based delivery systems for sustainable agriculture, Int. J. Biol. Macromol., 77 (2015) 36–51.
[31] J. Ma, K. Fu, J. Shi, Y. Sun, X. Zhang, L. Ding, Ultraviolet-assisted synthesis of polyacrylamide-grafted chitosan nanoparticles and flocculation performance, Carbohydr. Polym., 151 (2016) 565–575.
[32] Y. Chen, J. Li, Q. Li, Y. Shen, Z. Ge, W. Zhang, S. Chen, Enhanced water-solubility, antibacterial activity and biocompatibility upon introducing sulfobetaine and quaternary ammonium to chitosan, Carbohydr. Polym., 143 (2016) 246–253.
[33] J. Sun, X. Ma, X. Li, J. Fan, Q. Chen, X. Liu, J. Pan, Synthesis of a cationic polyacrylamide under UV initiation and its flocculation in estrone removal, Int. J. Polym. Sci., 2018 (2018) 1–11.
[34] X. Li, H. Zheng, Y. Wang, Y. Sun, B. Xu, C. Zhao, Fabricating an enhanced sterilization chitosan-based flocculants: synthesis, characterization, evaluation of sterilization and flocculation, Chem. Eng. J., 319 (2017) 119–130.
[35] S. Naskar, S. Sharma, K. Kuotsu, Chitosan-based nanoparticles: an overview of biomedical applications and its preparation, J. Drug Delivery Sci. Technol., 49 (2019) 66–81.
[36] M.P.M. da Costa, M.C. Delpech, I.L. de Mello Ferreira, M.T. de Macedo Cruz, J.A. Castanharo, M.D. Cruz, Evaluation of single-point equations to determine intrinsic viscosity of sodium alginate and chitosan with high deacetylation degree, Polym. Test., 63 (2017) 427–433.
[37] X. Lu, Y. Xu, W. Sun, Y. Sun, H. Zheng, UV-initiated synthesis of a novel chitosan-based flocculant with high flocculation efficiency for algal removal, Sci. Total Environ., 609 (2017) 410–418.
[38] D. Wang, T. Zhao, L. Yan, Z. Mi, Q. Gu, Y. Zhang, Synthesis, characterization and evaluation of dewatering properties of

chitosan-grafting DMDAAC flocculants, Int. J. Biol. Macromol., 92 (2016) 761–768.
[39] M.S. Sivakami, T. Gomathi, J. Venkatesan, H. Jeong, S. Kim, P.N. Sudha, Preparation and characterization of nano chitosan for treatment wastewaters, Int. J. Biol. Macromol., 57 (2013) 204–212.
[40] L. Chen, Y. Sun, W. Sun, K.J. Shah, Y. Xu, H. Zheng, Efficient cationic flocculant MHCS-g-P(AM-DAC) synthesized by UV-induced polymerization for algae removal, Sep. Purif. Technol., 210 (2019) 10–19.
[41] Y. Liu, H. Zheng, Y. Wang, X. Zheng, M. Wang, J. Ren, C. Zhao, Synthesis of a cationic polyacrylamide by a photocatalytic surface-initiated method and evaluation of its flocculation and dewatering performance: nano-TiO_2 as a photo initiator, RSC Adv., 8 (2018) 28329–28340.
[42] Y. Sun, M. Ren, W. Sun, X. Xiao, Y. Xu, H. Zheng, H. Wu, Z. Liu, H. Zhu, Plasma-induced synthesis of chitosan-g-polyacrylamide and its flocculation performance for algae removal, Environ. Technol., 40 (2019) 954–968.
[43] C.K. Choo, X.Y. Kong, T.L. Goh, G.C. Ngoh, B.A. Horri, B. Salamatinia, Chitosan/halloysite beads fabricated by ultrasonic-assisted extrusion-dripping and a case study application for copper ion removal, Carbohydr. Polym., 138 (2016) 16–26.
[44] Y.S. Ryu, I. Kim, S.H. Kim, Effect of modified ZnO nanoparticle on the properties of polylactide ultrafine fibers, J. Appl. Polym. Sci., 136 (2019) 47446.
[45] X. Li, J. Zhu, Y. Pan, R. Meng, B. Zhang, H. Chen, Fabrication and characterization of pickering emulsions stabilized by octenyl succinic anhydride-modified gliadin nanoparticle, Food Hydrocolloids, 90 (2019) 19–27.
[46] Y. Gokce, B. Cengiz, N. Yildiz, A. Calimli, Z. Aktas, Ultrasonication of chitosan nanoparticle suspension: influence on particle size, Colloids Surf., A, 462 (2014) 75–81.
[47] L. Feng, H. Zheng, X. Tang, X. Zheng, S. Liu, Q. Sun, M. Wang, The investigation of the specific behavior of a cationic block structure and its excellent flocculation performance in high-turbidity water treatment, RSC Adv., 8 (2018) 15119–15133.
[48] L. Guo, M. Lu, Q. Li, J. Zhang, Y. Zong, Z. She, Three-dimensional fluorescence excitation-emission matrix (EEM) spectroscopy with regional integration analysis for assessing waste sludge hydrolysis treated with multi-enzyme and thermophilic bacteria, Bioresour. Technol., 171 (2014) 22–28.
[49] Z. Liu, M. Huang, A. Li, H. Yang, Flocculation and antimicrobial properties of a cationized starch, Water Res., 119 (2017) 57–66.
[50] N.G. Kandile, H.M. Mohamed, Chitosan nanoparticle hydrogel based sebacoyl moiety with remarkable capability for metal ion removal from aqueous systems, Int. J. Biol. Macromol., 122 (2019) 578–586.
[51] R.C. Goy, D. de Britto, O.B.G. Assis, A review of the antimicrobial activity of chitosan, Polímeros, 19 (2009) 241–247.
[52] A. Jafari, S. Hassanajili, M.B. Karimi, A. Emami, F. Ghaffari, N. Azarpira, Effect of organic/inorganic nanoparticles on performance of polyurethane nanocomposites for potential wound dressing applications, J. Mech. Behav. Biomed. Mater., 88 (2018) 395–405.